STATUS OF THE BEAM PROFILE MEASUREMENTS AT THE LHC

G. Trad*, G. Baud, E. Bravin, B. Dehning, M. Ferroluzzi, A. Goldblatt,
E. Piselli, F. Roncarolo, J. Storey, Q. Veyrat
CERN, Geneva, Switzerland

Abstract

During LS1, the various instruments for beam profile measurement at the LHC were upgraded to cope with the beam energy increase. In this contribution, a review of the status of the synchrotron radiation monitors, the beam gas ionization monitors, the beam gas vertex detector and the wirescanners will be presented alongside the assessment of the obtained performance. The new features implemented and the issues encountered during 2015's operation will be highlighted. Additionally, the interventions and improvements planned for the coming winter shutdown will be discussed.

INTRODUCTION

In the following, an overview of the beam profile measurements at the LHC is presented. The status of the Wire Scanners (WS), the synchrotron light monitors (BSRT), the ionization profile monitors (BGI) and the beam gas vertex detector (BGV) will be reviewed, focusing on the performance of these instruments in 2015 run after the upgrades they underwent in LS1.

WIRE SCANNERS

Wire scanners are the reference instruments for transverse beam size and emittance measurements in the LHC. They are also used for calibrating other devices, such as the BGI and the BSRT. Its working principle consists of a thin carbon wire moved across the beam at the speed of 1 m s^{-1}; the radiation produced by the interaction of the protons with the wire is observed by means of downstream scintillators coupled to Photo Multiplier Tubes (PMT). This charge deposition is proportional to the local density of the beam and is used to measure the beam density profile [1].

Several hardware changes were scheduled on the WS to tackle limitations observed in Run I and to enforce the robustness of the system:

- The few vacuum leaks, that were observed in the end of Run I, were related to the lifetime of the bellows that were getting closer to their design value of 10000 scans. New compensation springs and redesigned bellows (with enhanced lifetime) were installed in view of a more intense use of the WS in run II.

- For a safer operation, following some incidents of wires stuck in the vacuum chamber during a scan, a new motion card firmware was deployed aiming at solving safety critical issues that may lead to wire breakage.

- To improve the PMT linearity response avoiding saturation, the voltage divider was modified such as a higher charge is available to the PMT while scanning.

These modifications came along with a completely refurbished operational software with improved features on bunch selection, emittance evolution visualisation, machine optics selection, particle type recognition and predefined scan settings.

Dedicated studies were carried out to investigated the reliability of the measurements mainly the accuracy and the precision of the measured beam sizes.

Measurement Accuracy

Several factors could affect the WS measurements accuracy, and need to be studied in detail for a full characterisation and mitigation [2].

PMT saturation It was observed in Run I that the measured beam size was heavily dependent on the system working point, which is defined by the PMT gain and the selection of the neutral density (ND) filter in between the scintillator and the PMT. The measurements in 2015, following the modification of the voltage divider, show that the issue was cured: a change of 1000 V in the PMT voltage (with an adequate choice of ND filter) led to a beam size variation of less than 3%.

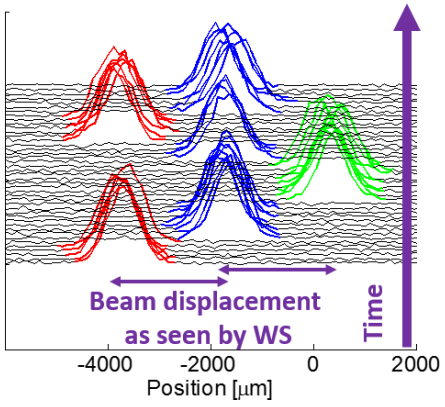

Figure 1: Beam profiles as measured by the WS during a closed orbit bumps scan of +/-2 mm with respect to the nominal orbit.

Scaling factors for wire position The wire position during a scan is measured by a potentiometer whose values are read by an ADC. The latter is calibrated by an optical ruler in the laboratory before the installation of the scanner

* georges.trad@cern.ch

Table 1: Discrepancy between the beam position monitors (in IR4) scale and the potentiometer scale for the LHC WS.

Scanner	Position Error	Emittance Error
B1H	3.6%	7.2%
B1V	2.7%	5.4%
B2H	4.5%	9.0%
B2V	3.3%	6.6%

in the accelerator. Any error on the absolute scale of the wire movement translates directly in an error on the measured beam size. Several tests were performed to crosscheck this scale by the mean of closed orbit bumps where the beam is moved by a known amount, as shown in Fig. 1 and its position is measured by the beam position monitors.

Ideally the beam movement seen by both the WS and the BPMs should match (accounting for the optics in the between the two instruments), however discrepancies are found and summarized in Tab. 1. The obtained corrections to apply to the WS scale were nevertheless not implemented since repeated measurements led to slightly different values and the absolute value of the error lays within the BPMs uncertainties. It is planned to investigate an alternative method in-situ to calibrate wire movement in the scanner via laser interferometry.

Crosstalk between bunches The limited bandwidth of the electronics handling the PMT signal (mainly the preamplifier in the tunnel) was found to introduce systematic errors to the bunch-by-bunch beam size measurements for trains of 25 ns spacing. These effects are seen as a crosstalk between bunches and are measured by filling single bunches in the machine and checking the artificial signals propagating in the adjacent slots. Under special conditions, where intensities and emittances of consecutive bunches are very different, the error on the obtained emittances can reach ~20%. For each operational scanner, a time constant modeling the signal decay across 25 ns bunch slots was retrieved, as in Fig.2, and will be used in 2016 as an input for a correction algorithm that was developed.

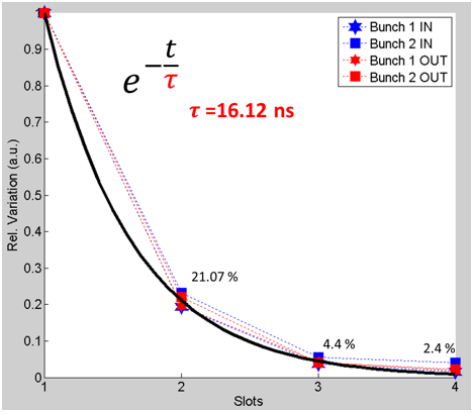

Figure 2: Measured decay of the signal amplitude of the BWS.5R4.B1H across the 25 ns slots, modeled and fitted exponentially.

Measurement Precision

Improving the measurement precision is important as well, especially when using WS for calibrating the other beam size measurement devices. In fact, for the BSRT case, WS precision is an important contributor to the systematics of the derived emittance. In 2015, large statistical fluctuation (>9%) of the measured emittance were observed from scan to scan, especially at top energy where the beam size is small. In this section we investigate effects of the noise coupled to the system on the WS measurements.

Noise on wire position reading Several hundreds of scans per device were analysed to check the mechanical reproducibility, by studying the wire movement as read by the potentiometer. The scans were found to be very reproducible, in terms of the fork acceleration, its speed during the scan and the deceleration. However the potentiometer reading was found noisy and affected by ~40 µm rms white noise. Simulations predicted that such a noise level would become an important limitation for scan to scan reproducibility, therefore it was proposed to neglect the wire position reading close by the beam interception and assume a constant speed by smoothing the wire position reading by a linear fit. This technique resulted very effective for B1 scanners where the measurements spread were reduced by factor 2-3 down to ~3%. Contrarily, this was not the case for B2 where no significant improvement was observed.

Noise on PMT signal readings The noise in the PMT signal acquisition chain was investigated by studying the spectrum of 100 scans with no beam in machine, as shown in Fig. 3. Noise can originate from the PMT High Voltage supplier or can be coupled to the analog signal in long cables or in the ADC chain. The present strategy to counteract this noise is the background subtraction, that consist of picking a bucket in the abort gap as a noise reference. It was proven that this technique would suppress the noise contribution

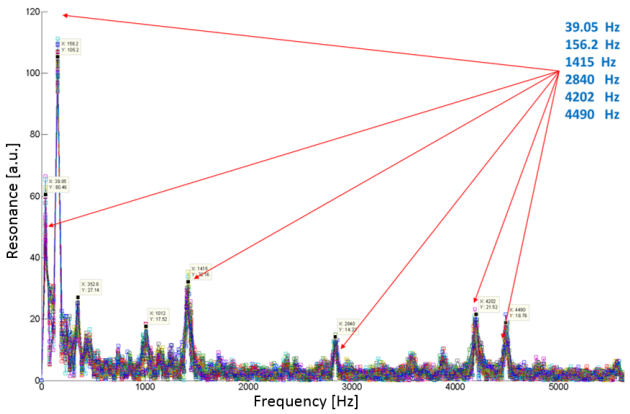

Figure 3: Noise spectrum of beam 1 PMT readings of 100 scans in absence of beam.

at low frequencies <1 kHz but unfortunately enhance the noise at higher frequencies. Suspected to contribute to the worsening of the WS precision, various options to suppress these noise lines at the hardware level are being investigated.

BEAM-GAS IONIZATION MONITOR

Four Beam-Gas Ionization monitors (BGI) (one per plane per beam) are installed in the LHC for emittance monitoring. The beam size is inferred by measuring the distribution of the electrons produced in the ionization process of the Neon gas injected into the vacuum chamber by the beam passage [3].

During LS1, the BGIs were completely dismounted. Maintenance operations were mainly carried out such as replacing the aging Multi Channel Plates (MCP) and installing temperature probes (only on B2 devices) to investigate suspected heating that could originate from electromagnetic interactions with the circulating beam. Additionally, to improve the system reliability and its lifetime, the radiation sensitive electronic components of the camera were relocated away from beam.

It is worth recalling that simulations and operational experience in Run I agree that with the present hardware no operation was foreseen for the protons run since the measurements were dominated by space charge effects and quite difficult to correct for [5].

The complete reassembly of the BGIs finished in 2015 TS3 just in time for the LHC operation with ions.

Operation with Ions

No beam time was requested for the BGI commissioning this year; however parasitically some studies were carried out. In the following only beam 1 devices will be discussed since unfortunately no signal was detected on beam 2 devices; investigations are still ongoing to check whether it is caused by communications problems or by camera lifetime issues.

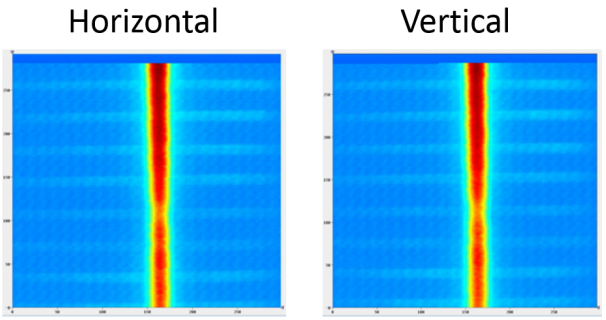

Figure 4: Beam 1 horizontal and vertical profiles as recorded by the BGI during the ion physics in Run II.

Figure 4, shows the recorded beam profiles (horizontal and vertical) by the BGI where a non-uniform Horizontal stripe was observed at the center of the image. Checking this non uniformity with the electron generation plates allowed to trace it back to the aging of the new MCPs.

Cross calibration with the BSRT

During a fill for ions physics, the beam emittance derived from the bunch emittances as measured by the BSRT and bunch intensity as measured by the fast beam current transformers were compared with the BGI measurements as shown in Fig. 5.

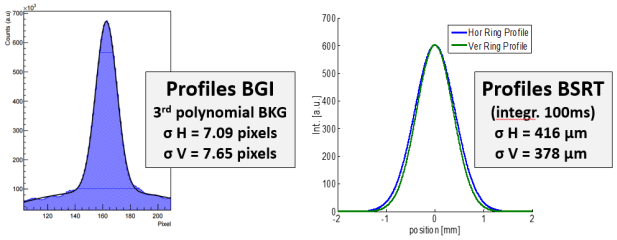

Figure 5: Cross-calibration of the BGI beam size (left) with respect to the beam profile measured by the BSRT (right).

Since the magnification of the optical system did not change, the same measured pixel size in Run I is used (~100μ/px). Consequently the calibration factors needed to correct the BGI measurements are found to be 580 µm and 690 µm for the horizontal and vertical plane respectively. These findings are coherent (at least in the horizontal plane) with predictions from 2015 extrapolations (PSF=500 µm) [4]. Further studies will be scheduled to measure precisely the magnification of the optical system by displacing the beam at the BGIs and study further the corrections to be applied.

Finally it is worth mentioning the unusual beam losses that were observed around the BGI (beam 1) that led to increasing the surrounding beam loss monitors threshold. The origin of such losses are still not identified and are being studied.

BEAM GAS VERTEX DETECTOR

A Beam-Gas Vertexing system (BGV) consisting of eight scintillating-fibre tracker modules was designed, constructed and installed by the end of TS3 in 2015 on LHC Ring 2 [6]. It will be operated as a pure non invasive beam diagnostics device. Its working principle, sketched in Fig. 6, consists of reconstructing the beam-gas interaction vertexes, where the charged particles produced in inelastic beam-gas interactions are measured with high-precision tracking detectors, to obtain the 2D beam transverse distribution.

The instrument is a demonstrator aiming to probe the potential of the beam-gas imaging technique for the LHC where. In this first phase, a full beam and b-by-b measurements are expected, also during ramp, however with modest requirements on the measurement time, precision and accuracy.

The beam size is obtained from the measurements after unfolding the instrument resolution, but the BGV is considered a self-calibrated monitor since the resolution can be measured from the data (track splitting method).

As a consequence, the main systematic error on the measured beam size comes from the vertex resolution that could

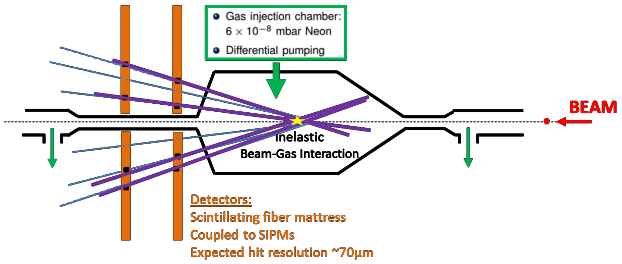

Figure 6: A sketch of the BGV Demonstrator layout. The two major components are shown: gas target (chamber for gas injection and accumulation, chambers with reduced aperture and pumping system) and tracking detector.

be compromised by the detector precision, and low track multiplicity. The latter is inversely proportional to the rate of "good" events.

The installed prototype is such as the expected rate of useful vertexes is ~1 Hz per nominal bunch. This is dictated by the choice of injected gas, its pressure, the radial distance from beam to the detector, the angular acceptance and the material budget. Such an event rate imply a measurement time of ~ five minute per bunch to reach a precision of ~ 4%, under the hypothesis of a Gaussian beam distribution.

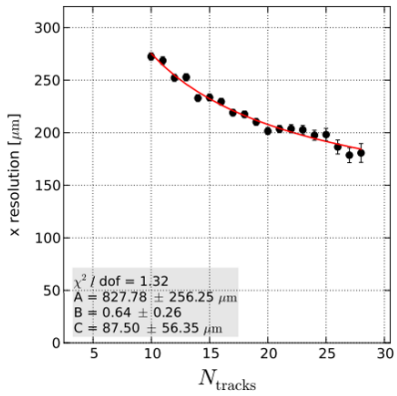

Figure 7: Achievable resolution of the present BGV demonstator in function of the tracks multiplicity.

In Run II, all the system components were checked with beam and both the detector and the readout were behaving as expected. The gas injection was commissioned however data was collected only with residual gas interactions. The data taking was mainly to verify the trigger latencies and for a preliminary temporal alignment of the vetos.

A problem was encountered with the BGV cooling system, where a slow diffusion of the cooling liquid through the silicon tubes was observed. At a later, cooling will become very important since it is meant to reduce higher dark current in the PMs caused by the increase of the accumulated dose. Therefore a redesign of the cooling system (i.e. the replacement of the existing tubes) is foreseen.

During the winter shutdown, YETS 2015, it is foreseen to install a light tight "tent" covering all the BGV and its scintillators to reduce the measurement background.

For the coming Run II, the commissioning of the system will consist of the acquisition of raw signals, develop the correction algorithms, the zero-suppressed readout track and vertex reconstruction. Finally an on-line application publishing and logging the beam size measurements and event data will be developed.

SYNCHROTRON LIGHT MONITOR

The Beam Synchrotron Radiation Telescope (BSRT) monitors image the synchrotron light generated by the beam traversing a dedicated super-conducting undulator and a D3 type dipole located in IR4. This section will cover the upgrade of the SR extraction system, the new cross-calibration technique with the WS and the updated performance of the new imaging system. Moreover, the effect of the machine optics on the BSRT measurements will be briefly discussed. Finally, two SR projects under development will be presented: the interferometer and the coronagraph, for the measurement of the beam size and the beam halo respectively.

SR extraction system

The show stopper for a reliable beam size measurement via SR imaging in the LHC Run I was the light extraction system. The electromagnetic coupling with the beam lead to the mirror heating, the deterioration of its coating and ultimately to the mechanical failure of its support. In LS1, a new holder for the in-vacuum extraction mirror, featuring smoother transitions in the beam pipe and consequently a much lower longitudinal impedance, was designed. The silicon bulk mirror was replaced by a dielectric coated glass bulk mirror to reduce the absorbed heat and consequently the coating deformation [7]. During the intensity ramp up in the LHC beam commissioning at the start of Run II, the temperature of the extraction mirror was closely monitored via in-vacuum probes installed on the mirror holder. No significant heating was observed, confirming the results of the simulations and laboratory test.

SR Imaging

Near Ultra-violet imaging At high energies, the radiation emitted by the dipole is broadband. Since the effects of diffraction can be reduced by using short wavelength SR improving the resolution and leading to more accurate measurements, a Near Ultra-Violet (NUV) imaging system, with lenses optimized for operation at 250 nm was installed alongside the existing imaging system optimized for operation at 600 nm. The optical resolution improvement was verified via the new cross calibration technique with the WS and the correction factors resulted about 10 to 15% lower than for the visible system.

Beam size calibration The beam size σ_{Beam} is extracted from the BSRT measurements ($\sigma_{BSRT_{meas}}$) by applying a correction in quadrature, assuming a Gaussian Line

Spread Function (σ_{LSF}) as the resolution of the optical system:

$$\sigma_{Beam} = \sqrt{{\sigma_{BSRT_{meas}}}^2 - {\sigma_{LSF}}^2} \quad (1)$$

The correction is the result of the convolution of the broadening caused by diffraction, the depth of field in the dipole and geometric/chromatic aberrations. This is calculated through calibration with the WS measurements. A new calibration technique [8] was used, allowing both the magnification K and resolution (σ_{LSF}) of the optics to be extracted from the cross-calibration with the WS. The former is derived from the slope and latter from the offset of a linear regression in terms of ${\sigma_{BSRT_{meas[px]}}}^2$ and ${\sigma_{WS[mm]}}^2$:

$${\sigma_{BSRT_{meas\,[px]}}}^2 = \left(\frac{\frac{\beta_{BSRT}}{\beta_{WS}}}{K}\right){\sigma_{WS\,[mm]}}^2 + {\sigma_{LSF\,[px]}}^2 \quad (2)$$

with β_{BSRT} and β_{WS} being the beta functions at the SR source and the WS respectively. The full calibration process includes scanning both the focusing lens and the camera searching for the combination featuring the lowest σ_{LSF}. A typical result map is shown in Fig. 8 (top right) where the focus can easily be found. Figure 8 shows also the evolution of the normalized emittances for two bunches over a large range as measured by the WS and the BSRT indicating the validity of this calibration procedure. This calibration

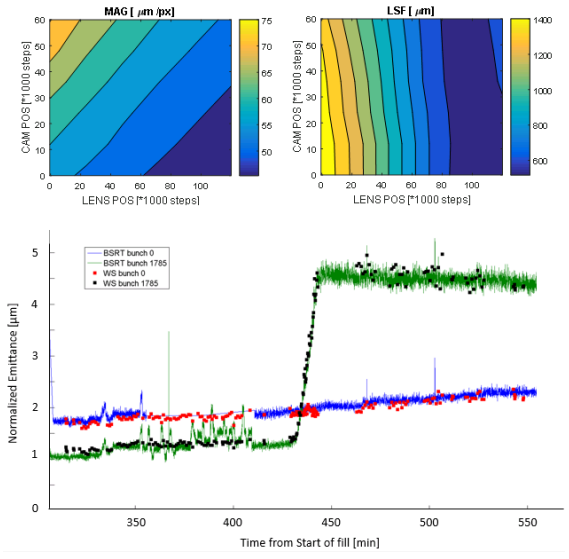

Figure 8: Top: BSRT Optical magnification and resolution for various combinations of lens and camera. Bottom: Emittance evolution as measured by the WS and a calibrated BSRT.

technique does not require slow closed orbit beam bumps to calculate the optical magnification and will allow for a calibration "on the fly" during the energy ramp, producing an energy dependent correction curve that can be used to measure the beam size from 2 TeV, once the visible SR is emitted exclusively by the bending dipole.

Machine Optics Effects

A good knowledge of the beta functions at the SR source and the WS is fundamental for a good characterization of the optical system. A very good accuracy was obtained following the K-modulation measurements on the standalone quadrupoles in IR 4, that contributed to the accuracy of the BSRT emittance measurement. However recent simulations showed that a dynamic beta beating is introduced in physics fills by beam-beam effects (mainly Head On collisions) and the beta function at the location of the BSRT could be changed up to 5%. Therefore, these effect should be accounted for when comparing the BSRT emittances with emittances derived from other techniques such as luminosity scans.

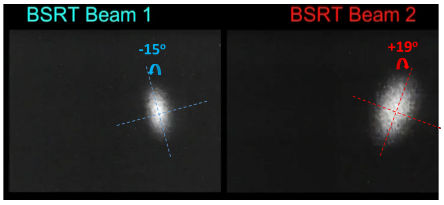

Figure 9: Tilted SR ellipses for blown up bunches, evidence of local linear coupling at the D3 dipole left and right of IP 4.

Recent observations during beam collimation studies, when the beams are blown up on purpose in one plane, show that the coupling is not perfectly corrected at the BSRT. In fact, as shown in Fig. 9 the beam ellipse resulted tilted by few degrees. This implies an error on the beam size determination that becomes particularly relevant for not round beams (i.e. large difference between horizontal and vertical beam sizes).

Performance in Run II

In 2015, the BSRT resulted reliably operational for bunch-by-bunch measurements. It has been crucial for several studies (beam-beam, instabilities and EC studies). Crosschecks with independent emittance measurements, such as the luminosity scans, confirmed the accuracy of the BSRT beam size measurement, found to be at the level of 5%. The stability of the system was also mainly driven by the improved FESA Server that is continuously being upgraded and optimized.

Future Upgrades

SR Imaging

Studies are foreseen to improve the BSRTS/WS cross-calibration by reducing the uncertainties on WS measurements (mainly noise studies). Investigations are also in place to identify the source of the big spread in the beam size measurement observed on BSRT B1V. With the increase of the number of bunches in the machine, the limited time at injection and the limited acquisition speed (3-5 bunches per second), the main challenge for Run II is to increase the BSRT bunch scan. This is planned to take place at two stages, where in the beginning the present frame grabber (BTV card)

would be replaced by a faster one (SVEC + 100MHz ADC) that will boost scan speed by factor 2-3. Nevertheless the final aim will be, in the framework of the BSRT consolidation, to switch to digital cameras featuring acquisitions up to some 100s frames per second. This upgrade would also include new intensifiers higher sensitivity and higher signal to noise ratio. This hardware improvement will be closely followed by software changes including porting the BSRT server to FESA3.

SR Interferometry

Direct imaging for beam size measurement, as explained above, is ultimately diffraction limited and is very sensitive to cross-calibrations. The interferometry technique, described in [9], is the best alternative to measure the beam size with visible SR. It consists of determining the size of a spatially incoherent source by probing the spatial distribution of the degree of coherence after propagation, with an achievable resolution of a few microns. Based on the findings in [8], where the instrument was fully characterized, a prototype was installed for measuring the vertical beam size on one of the LHC beams.

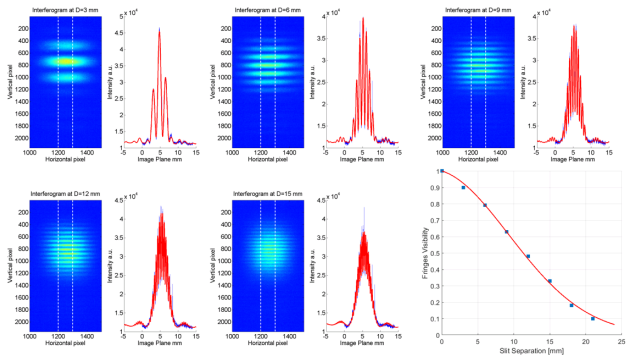

Figure 10: Interferograms and fringe visibility obtained at various double slit separation.

The visibility of the interferogram fringes, using the intensities I_{max} at the peak of the interference fringe and I_{min} at its valley, is defined as:

$$V = \frac{I_{max} - I_{min}}{I_{max} + I_{min}} = \frac{2\sqrt{I_1 \cdot I_2}}{I_1 + I_2} |\Gamma| \qquad (3)$$

where I_1 and I_2 are the light passing through the first and the second slit respectively. Figure 10 shows the results of a beam size measurement where the intensity pattern is recorded for varying slit separation D. Accounting for the intensity imbalance factor leads to the curve $|\Gamma(D)|$ that allows the reconstruction of the vertical beam distribution according to the Van Cittert-Zernike theorem [9].

Preliminary measurements showed that the interferometer systematically predicts a beam size that is 30-35% smaller than what measured by WS (and transported at the SR monitor location). Beam size overestimation can normally be attributed to source movement, air turbulence, noisy optical system, chromatic aberration or incoherent depth of field effects, but it is harder to explain this underestimation. An additional de-focusing deformation in the SR path before the slits, detector non linearity, bad background subtraction and different linear coupling values at the SR source and the WS are all being investigated to explain this underestimated beam size.

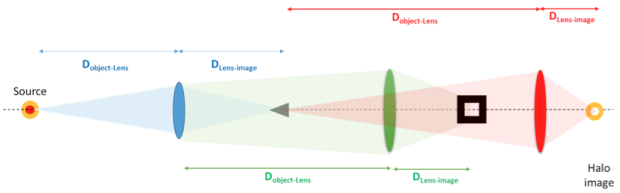

Figure 11: Sketch of the coronagraph prototype optical system showing the three fundamental focusing stages, the mask used to block the SR core and the Lyot stop (rectangular slit) to mask the diffraction fringes.

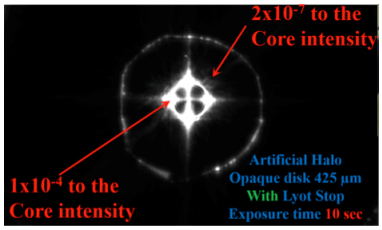

Figure 12: Measured diffraction pattern at the final stage of the coronagraph installed in the laboratory, confirming the leakage of the main diffraction fringes to be in the order of 10^{-4} with respect to beam core.

Halo measurement

The coronagraph is a spatial telescope used to observe the sun corona by creating an artificial eclipse. The concept of this apparatus, sketched in Fig. 11, consists of blocking the glare of the sun central image allowing to observe a its corona. An SR coronagraph for the observation of surrounding structure (halo, tail) of the beam was similarly developed for the Photon Factory at the KEK in 2004 [10], where an opaque disk placed at the beam image plane is used to block the bright beam core image. An observation of the beam halo at the LHC using the coronagraph is planned in two phases. In its final design, an optimum optical system designed taking into account the LHC SR parameters, will reach 10^5 to 10^6 contrast to the beam core [11]; however in the first phase, the coronagraph will be designed using some optical components of the coronagraph constructed in KEK in 2004 and will allow a halo observation with 10^3 to 10^4 contrast.

Before installing prototype in B2 optical monitor line during EYETS 2015, a replica was built in laboratory to validate the diffraction analysis. Measurements agree very well with the simulations and confirm that the background in this coronagraph is dominated by the leakage of diffraction fringe and is estimated to be $\sim 3.7x10^{-4}$.

It is worth noting that this diffraction fringes originating from the relay lens square aperture are mainly localized in the horizontal and vertical medium plane as shown in Fig. 12. It is worth noting that distinguishing hidden beam halo image from diffraction fringes could be achieved by rotating the aperture pupil, that rotates accordingly the medium planes without perturbing the beam image and its halo. Parasitic studies are scheduled in 2016 to check the system alignment and validate the optical configuration. Dedicated studies and MD time will be requested to assess the coronagraph performance, its background and the achievable contrast.

CONCLUSIONS

The various refurbishment the LHC beam profile monitors underwent in LS1 were fundamental for the reliable and accurate measurements at 6.5 TeV in Run II.

In particular, the hardware modifications to the wirescanners and the Fesa server updgrades allowed a safer operation in 2015 and mitigated the PMT saturation problem heavily affecting the measurement accuracy in Run I. Investigating the WS measurements accuracy and precision in dedicated studies allowed to assess the accuracy to be better than 3% and the precision (rms spread) better than 9%. The low precision was caused mainly by the noise affecting the potentiometer and PMT readings and solutions were proposed to mitigate these effects and will be included in future upgrades of the Fesa server.

The BGI status was also reviewed for the Run II ions operation. A preliminary cross-calibration for BGI beam sizes with respect to the BSRT measurements for beam 1 allowed calculating the instrument point spread function that was found coherent with the predictions.Investigations are still taking place to identify the signal absence from beam 2 BGI, suspected to be caused by a communication problem.

The new BGV was also presented. The device installation finished in 2015 TS3, and will be finalized in EYETS by installing a light tight tent around the BGV detectors to reduce the measurements background. An issue was encountered with the cooling system where a slow diffusion of the cooling liquid through the silicon tubes was observed and an intervention is scheduled to solved it. The commissioning of the system is planned to take place in Run II.

Finally, the BSRT were reviewed. The imaging system was reliably used for beam size measurement in Run II operation. The cross-calibration of the BSRT with respect to the WS allowed quantifying the accuracy found to be better than 6%. The precision of the beam size measurements was studied and found to be around 4% for B2 and slightly higher for B1. Following these encouraging results and seen the potential time at injection that can be spared, a proposal to abandon the systematic WS checks at first injections is therefore presented. The SR interferometer prototype installed on beam 1 was also presented with the encouraging results obtained in Run II. Dedicated studies are scheduled for beam size determination from the interferograms fringes visibility.

REFERENCES

[1] J. Emery et al., PERFORMANCE ASSESSMENT OF WIRE-SCANNERS AT CERN, TUPF03, IBIC2013, Oxford (UK).

[2] G. Trad: SPS and LHC wire scanners studies, Emittance working group 26 Aug 2015, `https://indico.cern.ch/event/439436/`

[3] M. Sapinski et al., Status of Beam Gas Ionization Monitor, LHC Beam Operation Committee LS1 LBOC meeting, 10 July 2012.

[4] M. Sapinski et al., The First Experience with LHC Beam Gas Ionization Monitor, THPB61, IBIC2012, Tsukuba (Japan).

[5] M. Patecki et al., Analysis of LHC Beam Gas Ionization monitor data and simulation of the Electron transport in the detector, CERN-THESIS-2013-155.

[6] BGV TWiki Home `https://twiki.cern.ch/twiki/bin/view/BGV/WebHome`

[7] F. Roncarolo et al., ELECTROMAGNETIC COUPLING BETWEEN HIGH INTENSITY LHC BEAMS AND THE SYNCHROTRON RADIATION MONITOR LIGHT EXTRACTION SYSTEM, TUPFI063, IPAC2013, Shanghai (China).

[8] G. Trad, "Development and Optimisation of the SPS and LHC beam diagnostics based on Synchrotron Radiation monitors," Ph.D. thesis, Beams. Dept.,CERN, 2015.

[9] T. Mitsuhashi, "Beam Profile and Size Measurement by SR Interferometers", in Beam Measurement: Proceedings of the Joint US-CERN-Japan-Russia School on Particle Accelerators, Editors S-i. Kurokawa, S.Y. Lee, E. Perevedentsev and S. Turner, p. 399–427, World Scientific, Singapore (1999)

[10] T. Mitsuhashi, "Design and Construction of Coronagraph for Observation of Beam Halo", Proceedings of EPAC, Lucerne, Switzerland (2004)

[11] T. Mitsuhashi, "Design of Coronagraph for the Observation of Beam Halo at LHC", Proceedings of IBIC, Melbourne, Australia (2015)